JCI The Journal of Clinical Investigation

In vivo visualization and attenuation of oxidized lipid accumulation in hypercholesterolemic zebrafish

Longhou Fang, … , Sotirios Tsimikas, Yury I. Miller

J Clin Invest. 2011;121(12):4861-4869. https://doi.org/10.1172/JCI57755.

Technical Advance **Cardiology**

Oxidative modification of LDL is an early pathological event in the development of atherosclerosis. Oxidation events such as malondialdehyde (MDA) formation may produce specific, immunogenic epitopes. Indeed, antibodies to MDA-derived epitopes are widely used in atherosclerosis research and have been demonstrated to enable cardiovascular imaging. In this study, we engineered a transgenic zebrafish with temperature-inducible expression of an EGFP-labeled single-chain human monoclonal antibody, IK17, which binds to MDA-LDL, and used optically transparent zebrafish larvae for imaging studies. Feeding a high-cholesterol diet (HCD) supplemented with a red fluorescent lipid marker to the transgenic zebrafish resulted in vascular lipid accumulation, quantified in live animals using confocal microscopy. After heat shock–induced expression of IK17-EGFP, we measured the time course of vascular accumulation of IK17-specific MDA epitopes. Treatment with either an antioxidant or a regression diet resulted in reduced IK17 binding to vascular lesions. Interestingly, homogenates of IK17-EGFP–expressing larvae bound to MDA-LDL and inhibited MDA-LDL binding to macrophages. Moreover, sustained expression of IK17-EGFP effectively prevented HCD-induced lipid accumulation in the vascular wall, suggesting that the antibody itself may have therapeutic effects. Thus, we conclude that HCD-fed zebrafish larvae with conditional expression of EGFP-labeled oxidation-specific antibodies afford an efficient method of testing dietary and/or other therapeutic antioxidant strategies that may ultimately be applied to humans.

In vivo visualization and attenuation of oxidized lipid accumulation in hypercholesterolemic zebrafish

Longhou Fang,[1] Simone R. Green,[1] Ji Sun Baek,[1] Sang-Hak Lee,[1] Felix Ellett,[2,3] Elena Deer,[1] Graham J. Lieschke,[2,3] Joseph L. Witztum,[1] Sotirios Tsimikas,[1] and Yury I. Miller[1]

[1]Department of Medicine, UCSD, La Jolla, California, USA. [2]Cancer and Haematology Division, Walter and Eliza Hall Institute of Medical Research, Melbourne, Australia. [3]Australian Regenerative Medicine Institute, Monash University, Clayton, Victoria, Australia.

Oxidative modification of LDL is an early pathological event in the development of atherosclerosis. Oxidation events such as malondialdehyde (MDA) formation may produce specific, immunogenic epitopes. Indeed, antibodies to MDA-derived epitopes are widely used in atherosclerosis research and have been demonstrated to enable cardiovascular imaging. In this study, we engineered a transgenic zebrafish with temperature-inducible expression of an EGFP-labeled single-chain human monoclonal antibody, IK17, which binds to MDA-LDL, and used optically transparent zebrafish larvae for imaging studies. Feeding a high-cholesterol diet (HCD) supplemented with a red fluorescent lipid marker to the transgenic zebrafish resulted in vascular lipid accumulation, quantified in live animals using confocal microscopy. After heat shock–induced expression of IK17-EGFP, we measured the time course of vascular accumulation of IK17-specific MDA epitopes. Treatment with either an antioxidant or a regression diet resulted in reduced IK17 binding to vascular lesions. Interestingly, homogenates of IK17-EGFP–expressing larvae bound to MDA-LDL and inhibited MDA-LDL binding to macrophages. Moreover, sustained expression of IK17-EGFP effectively prevented HCD-induced lipid accumulation in the vascular wall, suggesting that the antibody itself may have therapeutic effects. Thus, we conclude that HCD-fed zebrafish larvae with conditional expression of EGFP-labeled oxidation-specific antibodies afford an efficient method of testing dietary and/or other therapeutic antioxidant strategies that may ultimately be applied to humans.

Introduction

Cholesterol-fed zebrafish represent a novel animal model in which to study the early events involved in vascular lipid accumulation and lipoprotein oxidation (1, 2). This zebrafish model has several unique advantages. The optical transparency of zebrafish larvae enables high-resolution monitoring of vascular pathology in live animals. Colony maintenance is cost-effective, and many embryos can be produced from a single mating. Further, it is relatively easy to establish new transgenic zebrafish lines harboring fluorescent proteins. Importantly, our recent work established that feeding zebrafish a high-cholesterol diet (HCD) resulted in hypercholesterolemia, vascular lipid accumulation, myeloid cell recruitment, and other pathological processes characteristic of early atherogenesis in mammals (1). HCD-fed zebrafish had remarkably high levels of oxidized lipoproteins and specific oxidized phospholipid and cholesteryl ester moieties as measured by binding of oxidation-specific antibodies and by mass spectrometry (1, 2). These observations suggest that there is accelerated lipid oxidation in HCD-fed zebrafish.

Oxidative modification of LDL is widely believed to drive the initial formation and progression of atherosclerotic lesions in humans and experimental animals (3). Oxidized LDL (OxLDL) is considered a strong proinflammatory component of atherosclerotic lesions, and the plaques that contain higher amounts of OxLDL are vulnerable to rupture (4). Oxidative modifications of LDL render it immunogenic, and "oxidation-specific epitopes" in OxLDL are recognized by antibodies of innate and adaptive immunity (5). A major family of biologically relevant oxidation-specific epitopes are moieties derived from malondialdehyde (MDA) (6). We cloned a number of MDA-specific antibodies, such as the murine monoclonal MDA2, which recognizes the MDA epitope in atherosclerotic lesions of humans and mice. The human monoclonal antibody IK17 was cloned from a human phage-display library and binds to MDA epitopes on MDA-LDL and OxLDL (7). Further, MDA2 and IK17 — as well as the murine monoclonal antibody E06, which is specific to oxidized phospholipids — have been conjugated to gadolinium-labeled micelles (8) or iron oxide particles (9) and used to image atherosclerotic lesions in live *Apoe*$^{-/-}$ mice using MRI technology. Since OxLDL-rich plaques are vulnerable to rupture (4), these studies showing molecular imaging applications of oxidation-specific antibodies in live animals are important for future development of clinical cardiovascular imaging techniques.

In addition to cardiovascular imaging applications, many of these oxidation-specific antibodies have the potential to be used as therapeutics to inhibit lesion formation. This is based on the observation that they bind to relevant epitopes on OxLDL that mediates uptake of OxLDL by macrophages. Thus, IK17 inhibits the binding and uptake of OxLDL by macrophages (7). We have also demonstrated that increasing titers of oxidation-specific antibodies, and thereby neutralizing OxLDL in vivo, can reduce

Authorship note: The laboratories of Joseph L. Witztum, Sotirios Tsimikas, and Yury I. Miller contributed equally to this work.

Conflict of interest: Sotirios Tsimikas and Joseph L. Witztum are named as inventors on patents and patent applications for the potential commercial use of antibodies to oxidized LDL held by UCSD. Yury I. Miller is named as inventor on patents and patent applications for the potential commercial use of hypercholesterolemic zebrafish held by UCSD.

Citation for this article: *J Clin Invest.* 2011;121(12):4861–4869. doi:10.1172/JCI57755.

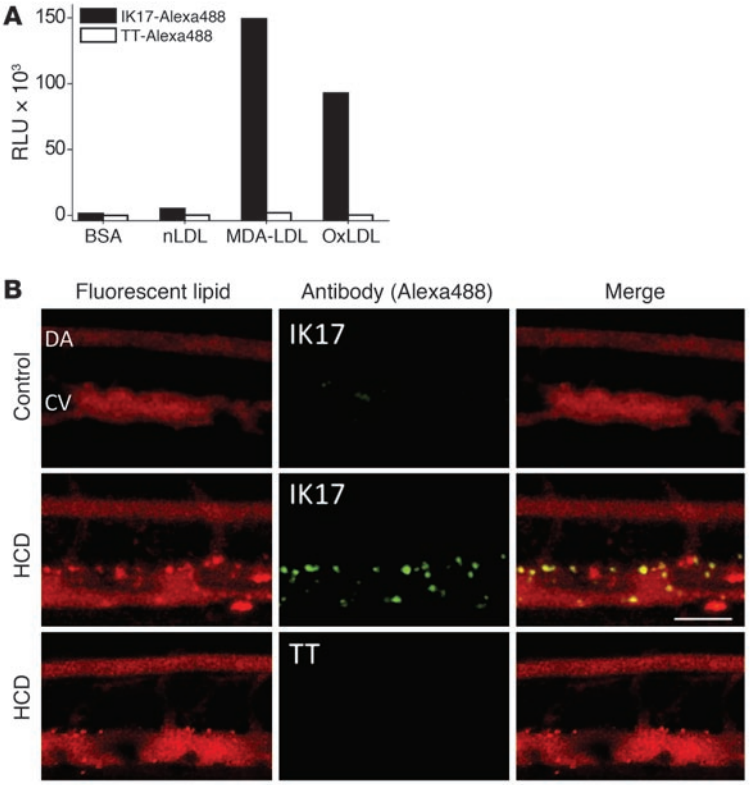

Figure 1
Binding of recombinant IK17 to vascular lipid deposits in HCD-fed larvae. (**A**) Binding of fluorescently labeled IK17-Alexa488 and TT-Alexa488 to MDA-LDL and OxLDL was tested in a microplate immunoassay with anti-HA antibody detection, as described in Methods. Two independent experiments were performed in quadruplicates. nLDL, native LDL. (**B**) Zebrafish larvae were fed a HCD or control diet supplemented with 10 μg/g cholesteryl BODIPY 576/589 C11 for 14 days. At the end of the feeding period, larvae were injected into the caudal vein with 2 nl 10 ng/μl IK17-Alexa488 or TT-Alexa488. Twenty-four hours after injection, larvae were anesthetized and imaged live under a confocal microscope. Lipid deposits (bright red) and sites of IK17-Alexa488 binding (green) partially colocalize (yellow) in the wall of the caudal vein. Diffuse red fluorescence in the lumen is from circulating lipid marker associated with plasma lipoproteins; its intensity varies depending on the cholesterol content in diet. DA, dorsal aorta; CV, caudal vein. Scale bar: 25 μm. Representative images from 4 animals in each group.

the atherosclerosis burden in mice and rabbits and, thus, could be used as a therapeutic method (10–13).

In the current work, we tested an approach that we believe to be new to image oxidation-specific epitopes on a microscopic level in a live animal, using conditional expression of an oxidation-specific antibody in zebrafish larvae. We present evidence that conditional expression of a functional single-chain IK17 antibody enables the time course measurements of vascular accumulation of oxidation-specific epitopes and the assessment of therapeutic effects of antioxidants and regression diets. Moreover, we demonstrate that sustained expression of IK17, which likely neutralizes oxidation-specific epitopes, has the therapeutic effect of reducing vascular lipid accumulation.

Results

Imaging vascular lesions with injected recombinant IK17. The Fab fragment of IK17 was converted into a biologically functional single-chain antibody (scFv), as described in Methods. The recombinant IK17-scFv (hereafter referred to as IK17) was labeled with Alexa Fluor 488 (referred to as IK17-Alexa488) and purified to remove endotoxin. As a negative control, we used a human scFv to tetanus toxin (referred to as TT). After labeling, binding of IK17-Alexa488 to MDA-LDL and OxLDL was validated in ELISA (Figure 1A). TT labeled with Alexa Fluor 488 (TT-Alexa488) did not bind to these modified LDL.

Zebrafish larvae were fed a control diet or HCD for 14 days prior to injection with labeled antibody. As we reported earlier (1), feeding zebrafish a HCD leads to hypercholesterolemia. Adding cholesteryl BODIPY 576/589 C11 to the HCD or control diet resulted in the appearance of diffuse red fluorescence in the vasculature (ref. 1, Figure 1B, and Supplemental Figure 1; supplemental material available online with this article; doi:10.1172/JCI57755DS1); its intensity varied depending on diet. Bright red spots on the caudal vein and less frequently on the dorsal aorta mark lipid deposits in the vascular wall (1). We previously reported that feeding *lyz:DsRed2* zebrafish a HCD resulted in recruitment of myeloid cells to the vasculature (1). Here, we used *mpeg1:EGFP* zebrafish, in which macrophages express EGFP (14), to demonstrate that vascular macrophages accumulate lipid. As shown in Supplemental Figure 2, red fluorescent lipid was found inside green fluorescent macrophages. Some lipid deposits were not associated with macrophages. These results agree with the human and mouse data, showing that, in the vascular wall, lipid accumulates in macrophages and in other cell types (e.g., vascular smooth muscle cells) and is also bound in the extracellular matrix (3). Since red BODIPY fluorophore is on the acyl chain of the cholesteryl ester, which is likely hydrolyzed in the digestive system, and the fluorescent fatty acid is then reesterified into cholesteryl esters, triglycerides, or phospholipids, the red fluorescence represents all classes of lipids. In a separate experiment, we added NBD-labeled free cholesterol to a HCD and observed its accumulation in the vascular wall as well (Supplemental Figure 3).

IK17-Alexa488 or TT-Alexa488 was injected into the posterior cardinal vein, as shown in Supplemental Figure 4. Twenty-four hours later, the zebrafish were imaged in the caudal vein area (Supplemental Figure 4), which was a different area from that of the site of injection. IK17 visibly bound to selected areas of lipid deposits in the vascular wall of HCD-fed, but not control, zebrafish (Figure 1B). There was insignificant binding of TT to the vasculature. The results showing binding of injected labeled IK17 to vascular lesions in larvae agree with IK17 staining of frozen sections of adult zebrafish, which was competed out by addition of MDA-LDL (Supplemental Figure 5). The fact that there was incomplete colocalization of lipid (red) and IK17 (green) signals in larvae (Figure 1B) suggests

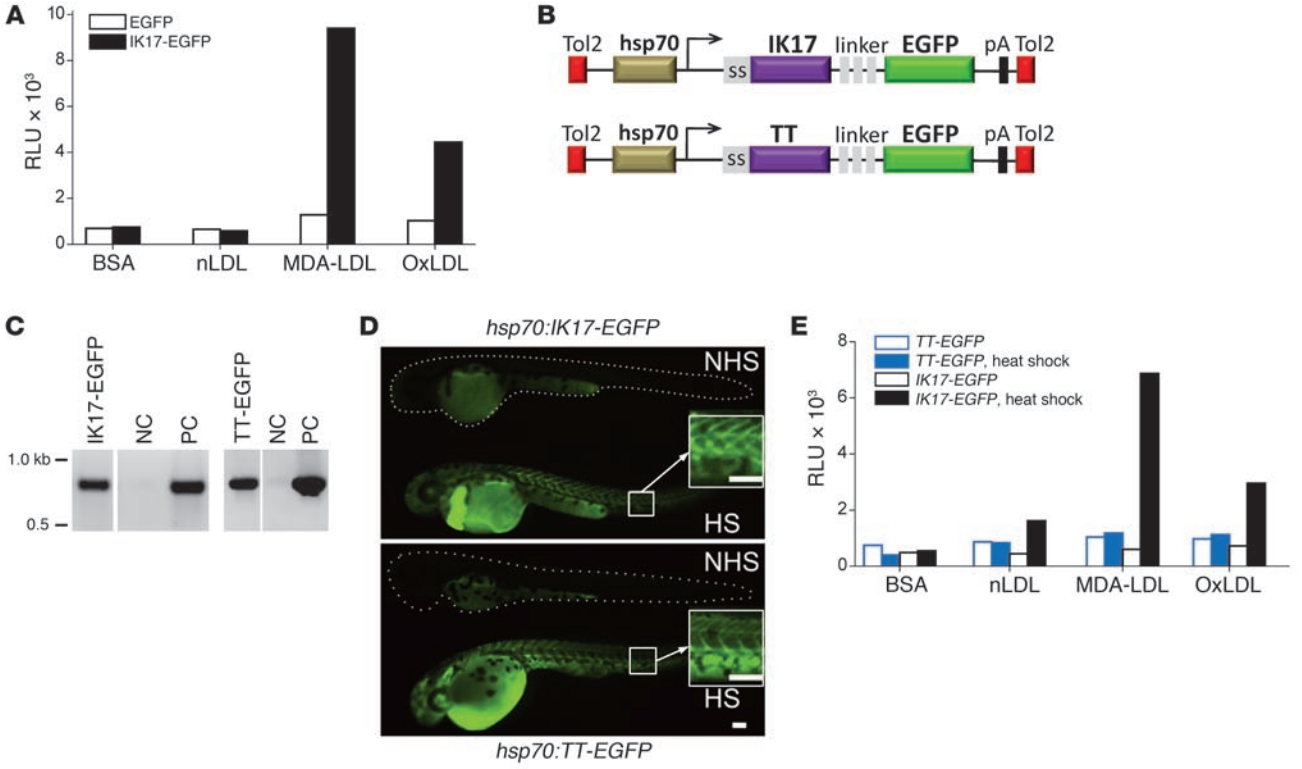

Figure 2

Transgenic *hsp70:IK17-EGFP* and *hsp70:TT-EGFP* zebrafish. (**A**) HEK293 cells were transiently transfected with EGFP or IK17-EGFP, and 48 hours after transfection, the supernatants were analyzed for binding with MDA-LDL and OxLDL in a microplate assay with an anti-GFP detection antibody. Two independent experiments were performed in quadruplicates. (**B**) Diagram showing the *hsp70:IK17-EGFP* and *hsp70:TT-EGFP* constructs used to generate transgenic lines. Tol2, a transposable DNA element; ss, secretion signal; pA, polyA sequence. (**C**) Founder *hsp70:IK17-EGFP* and *hsp70:TT-EGFP* zebrafish were genotyped with IK17 and TT primers. The hairline splices denote lanes that were run on the same gel but were noncontiguous. NC, negative control; PC, positive control. (**D**) Two dpf F_1 larvae of *hsp70:IK17-EGFP* and *hsp70:TT-EGFP* zebrafish were subjected to heat shock (HS). EGFP fluorescence was accessed 24 hours after heat shock. NHS, the larvae that were not subjected to heat shock. Dotted lines trace contours of the larvae that were not subjected to heat shock. Scale bar: 100 μm. (**E**) One group of 3 dpf *hsp70:IK17-EGFP* and *hsp70:TT-EGFP* larvae was subjected to heat shock, while the other group was not subjected to heat shock. Two days later, 30 fish from each group were homogenized; the homogenates were cleared by centrifugation and filtration, diluted 1:50, and tested for binding to MDA-LDL and OxLDL in a microplate assay with an anti-GFP detection antibody. Two independent experiments were performed in quadruplicates.

that MDA epitopes accumulate only in selected areas of vascular lesions. This selective accumulation of IK17-specific epitopes in zebrafish vasculature agrees with the selective IK17 staining of mouse and human atherosclerotic lesions (7).

Transgenic zebrafish with conditional expression of IK17-EGFP. Generation of a transgenic zebrafish that conditionally expresses a functional scFv of IK17 has numerous advantages compared with injection of recombinant antibodies, including (a) avoiding the necessity to produce and purify antibodies and to test the quality and purity of each preparation, including avoidance of problems with endotoxin contamination; (b) avoiding traumatic intravenous injections into tiny larvae; (c) providing the ability to simply and efficiently control transient antibody expression repeatedly and at specified time points, thus facilitating temporal studies; and (d) providing the ability to study therapeutic effects of diets, antioxidants, and oxidation-specific antibodies themselves, without repetitive injections of recombinant antibody.

We subcloned IK17-scFv and TT-scFv into pEGFP-N1 with a 39–amino acid linker inserted between IK17-scFv (or TT-scFv) and EGFP to better accommodate the antibody activity, and expressed these vectors in HEK293 cells. Testing the supernatants, we confirmed that the IK17-EGFP chimera bound to MDA-LDL and OxLDL and that TT-EGFP did not (Figure 2A and Supplemental Figure 6). Next, IK17-EGFP was cut out of the original vector and ligated into a mTol2 vector downstream of the zebrafish heat shock cognate 70-kd protein (*hsp70*) promoter (Figure 2B). The *hsp70* promoter conditions the expression of IK17-EGFP in response to heat shock (placing larvae for 1 hour in water at 37°C; normal water temperature for zebrafish maintenance is 28°C). Hsp70-driven expression of target genes has been described (15). The constructs were used to establish stable *hsp70:IK17-EGFP* and *hsp70:TT-EGFP* transgenic lines (Figure 2, C and D). In an ELISA experiment, we used homogenates of *hsp70:IK17-EGFP* subjected to heat shock to confirm that larvae produced functional IK17-EGFP that bound to MDA-LDL and OxLDL (Figure 2E). Furthermore, we used IK17 Fab and homogenates of IK17-EGFP–expressing zebrafish larvae to compare affinity of these antibodies in an ELISA-based competition assay (Supplemental Figure 7). The dissociation constants (K_d) for IK17 Fab and IK17-EGFP were 9.6×10^{-8} and 2.1×10^{-8} mol/l, respectively, demonstrating that the single-chain

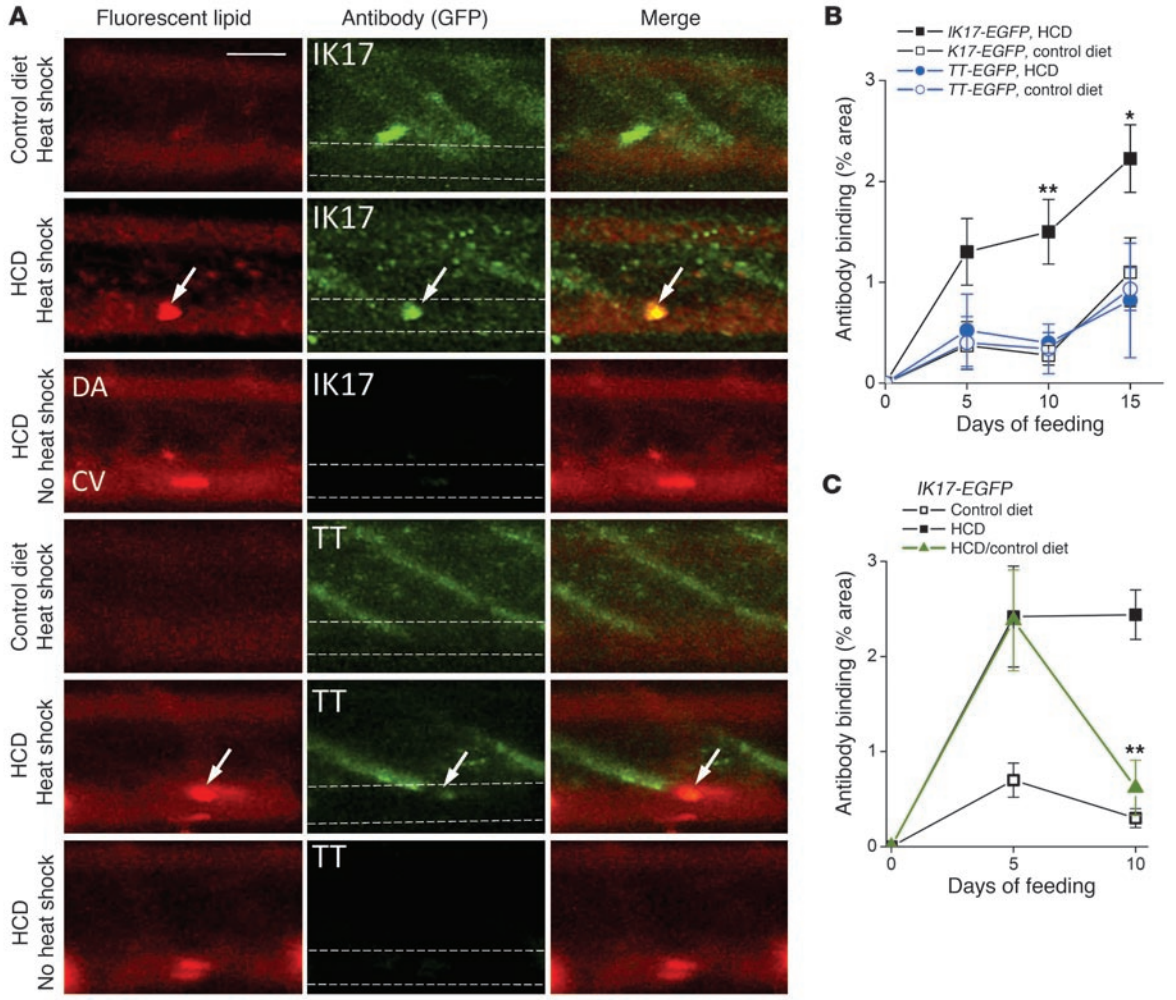

Figure 3

IK17-EGFP binding to vascular lipid deposits in HCD-fed transgenic larvae — time course and effect of dietary intervention. (**A**) *hsp70:IK17-EGFP* and *hsp70:TT-EGFP* zebrafish larvae were fed a HCD for 3 days, followed by heat shock (1 hour at 37°C) and 2 more days of feeding with a HCD supplemented with cholesteryl BODIPY 576/589. Control groups were fed either control diet and subjected to heat shock or fed HCD but not subjected to heat shock. Colocalization of green EGFP and red lipid marker signals was observed only in HCD-fed *hsp70:IK17-EGFP* subjected to heat shock (arrows). Dashed lines trace the caudal vein in GFP-only images. Scale bar: 50 μm. Representative images from 5–6 animals in each group. (**B**) The time course of IK17-EGFP and TT-EGFP binding. Transgenic zebrafish larvae were fed a HCD or control diet for the indicated number of days. Two days before imaging, fish were subjected to heat shock, and the diet was switched to a diet supplemented with cholesteryl BODIPY 576/589. Different groups of larvae were used for each time point. The results are expressed as the percentage of the area of EGFP signal normalized to the area of the caudal vein segment. Mean ± SEM (5–15 animals in each group at each time point).*$P < 0.05$; **$P < 0.01$. (**C**) One group of larvae was fed a HCD for 10 days, and the other group was fed a HCD for 5 days, followed by control diet for next 5 days. Mean ± SEM (13–18 animals in each group at each time point). **$P < 0.01$.

IK17-EGFP fusion expressed in zebrafish is as efficient an antibody as the parent IK17 Fab in recognizing the MDA epitope.

Imaging temporal and treatment-dependent changes in vascular binding of IK17-EGFP. Upon heat shock, both *hsp70:IK17-EGFP* and *hsp70:TT-EGFP* larvae rapidly expressed EGFP in somites, while there was no noticeable EGFP signal from the cells in the vascular wall (Figure 2D and Figure 3A). This was to our advantage, as we could now separate the signal from IK17-EGFP–producing tissues and the signal from the sites in which secreted IK17-EGFP bound to its specific epitopes. Twenty four hours after heat shock, accumulation of IK17-EGFP in the vascular wall of larvae fed a HCD was already noted. The images in Figure 3A show IK17-EGFP and TT-EGFP expression in zebrafish tissues after 48 hours after heat shock and, importantly, binding of secreted IK17 to lipid deposits in the vascular wall. There was no specific binding of secreted TT in the areas of vascular lipid deposition. Punctate IK17-EGFP fluorescence in somites of HCD-fed larvae subjected to heat shock may represent accumulation of IK17-reactive epitopes in small blood vessels and/or intermuscular lipid deposits. We have also confirmed with wild-type (AB) larvae that heat shock per se does not affect vascular lipid accumulation (Supplemental Figure 8).

Further, we measured areas of IK17-EGFP vascular binding on the fifth, tenth, and fifteenth days after the start of HCD or control diet feeding. The graph in Figure 3B shows the time course

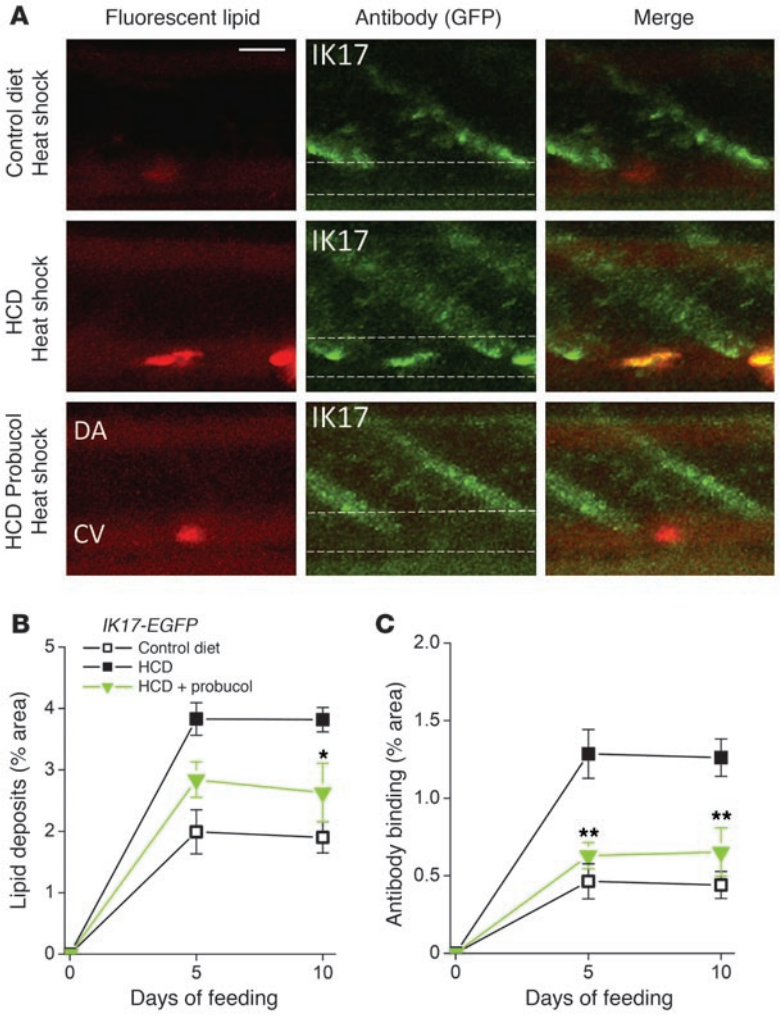

Figure 4
Effect of probucol on vascular lipid accumulation and IK17-EGFP binding in HCD-fed transgenic larvae. *hsp70:IK17-EGFP* zebrafish larvae were fed control diet, HCD, or HCD supplemented with 0.05% probucol. Other conditions were as in Figure 3. (**A**) Images of vascular lipid deposits and IK17-EGFP binding after 5 days of feeding. Dashed lines trace the caudal vein in GFP-only images. Scale bar: 25 μm. (**B**) Area of lipid deposits normalized to the area of the caudal vein segment. (**C**) IK17-EGFP binding expressed as the percentage of the area of EGFP signal normalized to the area of the caudal vein segment. Mean ± SEM (10–23 animals in each group at each time point). $^*P < 0.05$. $^{**}P < 0.01$.

of accumulation of IK17-reactive oxidation-specific epitopes over the course of HCD feeding, with a more than 5-fold increase in HCD-fed zebrafish over that in the control by the tenth day. The TT-EGFP binding did not differ between HCD-fed and control larvae. These data demonstrate that the HCD-induced vascular lipid accumulation was accompanied by enhanced accumulation of oxidation-specific epitopes. On average, 33% ± 14% of vascular lipid deposits were positive for IK17-EGFP binding.

To test the utility of measuring IK17-EGFP vascular binding, we performed short-term regression diet (Figure 3C) and antioxidant treatment (Figure 4) experiments. One group of animals was fed a HCD for 10 days, and a different group was fed a HCD for 5 days and then switched back to control diet for another 5 days. Vascular IK17-EGFP binding — high on the fifth day — was reversed after the dietary switch, reaching the levels observed in the group that received the control diet for the whole 10-day period (Figure 3C).

We have previously shown that probucol is a robust lipophilic antioxidant that can potently decrease atherogenesis in rabbits independent of changes in plasma cholesterol levels (16, 17). To determine whether probucol could inhibit vascular lipid deposition and/or oxidized lipid formation in HCD-fed zebrafish also, we added probucol to the HCD and measured vascular lipid accumulation and IK17-EGFP binding in larvae on the fifth and tenth days of feeding. Representative images are shown in Figure 4A and Supplemental Figure 9. The areas of lipid deposits were significantly lower in the group supplemented with probucol than in the group fed a regular HCD (Figure 4B and Supplemental Figure 10). The reduction in the vascular lesions to which IK17-EGFP bound was even more profound (Figure 4C), with many lipid deposits devoid of IK17-reactive epitopes (as in bottom panels of Figure 4A). Probucol did not affect IK17-EGFP expression in somites (Supplemental Figure 11).

IK17 expression inhibits vascular lipid accumulation. Next, we tested the hypothesis that constitutive expression of IK17 in zebrafish would attenuate vascular lipid deposition. This hypothesis is based on the observation that the IK17 Fab can bind to relevant MDA-like epitopes and prevent MDA-LDL binding to macrophages as well as its uptake (7). Our prior demonstration that raising the titers of antibodies to MDA-LDL by immunization or by adenovirus-delivered expression of IK17 was atheroprotective in rabbits and mice (10, 11, 13, 18) is consistent with this hypothesis.

We now demonstrate that the recombinant IK17-scFv, but not TT-scFv, inhibited binding of biotinylated MDA-LDL to murine macrophages (Figure 5A). All zebrafish larvae homogenates also competed to some degree with MDA-LDL binding to macrophages, consistent with our earlier findings of zebrafish homogenates binding to macrophages (2). However, only homogenates of transgenic zebrafish expressing IK17-EGFP specifically inhibited binding of MDA-LDL to macrophages at markedly lower concentrations than those of TT-EGFP homogenates and homogenates of larvae not subjected to heat shock (Figure 5B). These results suggest that in vivo IK17 expression may have a therapeutic effect.

To test this hypothesis, we subjected *hsp70:IK17-EGFP* zebrafish to repeated heat shocks to ensure sustained IK17-EGFP expression during the whole 10-day period of HCD feeding. The resulting levels of vascular lipid accumulation were dramatically reduced compared with the levels observed in HCD-fed *hsp70:IK17-EGFP* fish that were not subjected to heat shock (Figure 6A). Moreover, when heat shock was applied for the first time only on the fifth day after the start of HCD feeding, the ensuing IK17-EGFP expression reduced the area of lipid deposits measured 5 days later (Figure 6B). Expression of TT-EGFP did not change vascular lipid accumulation (Figure 6).

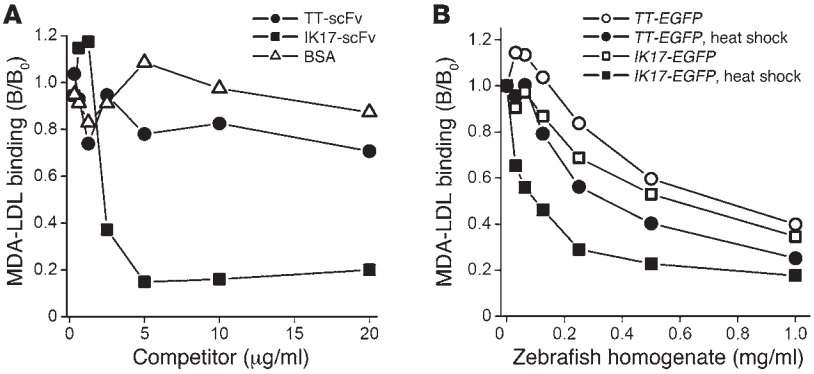

Figure 5
Zebrafish homogenates expressing IK17-EGFP inhibit MDA-LDL binding to macrophages. (**A**) In a macrophage binding experiment, binding of 0.15 μg/ml MDA-LDL to J774 cells was inhibited by indicated concentrations of IK17-scFv or TT-scFv. Two independent experiments were performed in triplicate. (**B**) The homogenates of *hsp70:IK17-EGFP* and *hsp70:TT-EGFP* zebrafish larvae (pooled from 50 animals in each group) that were used in the experiment shown in Figure 2E and at concentrations indicated were used to inhibit binding of 0.15 μg/ml MDA-LDL to J774 cells. Graphs are representative of 2 independent experiments, performed in triplicate.

Discussion

Lipoprotein metabolism in fish has many common features with lipoprotein metabolism in humans. VLDL, LDL, and HDL have been identified in fish using analytic ultracentrifugation (19). Although HDL dominates the lipoprotein profile in "normolipidemic" zebrafish, HCD feeding results in major increases in LDL and VLDL fractions (1). ApoE, apoB, apoA1, the LDL receptor, microsomal triglyceride transfer protein, lipoprotein lipase, hepatic lipase, and lecitin:cholesterol acyltransferase activities have been identified in fish (19, 20). Unlike mouse plasma, fish plasma displays cholesteryl ester transfer protein (CETP) activity (21), and the zebrafish *cetp* gene has been identified. In addition, dramatic increases in lipoprotein oxidation in HCD-fed zebrafish (1, 2), to a greater extent than those observed in any other animal model of atherosclerosis, make hypercholesterolemic zebrafish a particularly valuable model to study mechanisms and effects of lipoprotein oxidation.

Our earlier studies demonstrated increased plasma levels of oxidized phospholipids in HCD-fed adult zebrafish, as measured by the E06 immunoassay (1), and increased levels of oxidized phospholipids and oxidized cholesteryl esters in HCD-fed larvae, as measured by liquid chromatography-mass spectrometry (2). Similar to the MDA epitopes that are strongly expressed in human and mouse atherosclerotic lesions (22), we found IK17-reactive MDA epitopes in vascular lesions of adult and larval zebrafish (Figures 1, 3, and 4 and Supplemental Figures 5 and 9). Furthermore, in the zebrafish models, IK17 epitopes accumulate in vasculature as early as 5 days after the start of HCD feeding (Figure 3). Accumulation of vascular oxidation-specific epitopes in zebrafish was inhibited by the antioxidant probucol as well as by institution of a regression diet (Figures 3 and 4). The effect of a regression diet on the reduction of IK17 binding was evident as early as 5 days after the diet switch, compared with that of a regression diet mouse study (22) that was 6 months long. These data strongly support the HCD-fed zebrafish as a model in which enhanced lipid oxidation rapidly occurs in response to hypercholesterolemia. Furthermore, the use of the IK17-EGFP transgenic zebrafish allows one to quantify the accumulation of oxidation-specific epitopes on an ongoing basis in response to therapy. Since oxidation of LDL is thought to be a vital component of atherogenesis (23), zebrafish larvae with conditional expression of oxidation-specific antibodies afford an efficient method of testing dietary and/or other therapeutic interventions, as related to early stages of atherogenesis.

Our results further demonstrate that IK17 expression in zebrafish prevents vascular lipid accumulation (Figure 6A) and, remarkably, leads to regression of existing lipid deposits (Figure 6B), suggesting that at this early stage of vascular lipid accumulation, antibodies targeted to oxidation-specific epitopes are able to cause lesion regression. Because a single-chain antibody does not have an Fc fragment, it would not bind to cellular Fc receptors or to com-

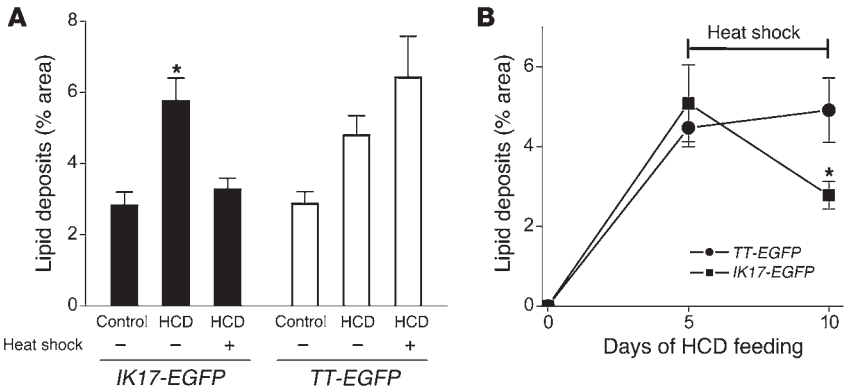

Figure 6
Expression of IK17-EGFP attenuates vascular lipid accumulation. (**A**) *hsp70:IK17-EGFP* and *hsp70:TT-EGFP* zebrafish larvae were fed a HCD or control diet for 10 days. One group of HCD-fed zebrafish was subjected to heat shock 2 days before the start of feeding and then every 4–5 days to sustain IK17-EGFP or TT-EGFP expression levels. The other group was not subjected to heat shock at any time and, thus, did not express the transgene. Two days before imaging, the diet was switched to a diet supplemented with 10 μg/g cholesteryl BODIPY 576/589 C11, and then fluorescent lipid deposits were quantified. The results are expressed as the percentage of the area of lipid deposits normalized to the area of the caudal vein segment. Mean ± SEM (21–34 animals in each *hsp70:IK17-EGFP* zebrafish group and 10–19 animals in each *hsp70:TT-EGFP* group). *$P < 0.001$ for IK17/HCD versus either IK17/control or IK17/HCD/heat shock. (**B**) Zebrafish larvae were fed a HCD for 5 days, and lipid deposits were imaged and quantified. The animals were subjected to heat shock after the imaging session on the fifth day and then again on the eighth day. The animals were imaged again on the tenth day, and lipid deposits were quantified. The results are expressed as the percentage area of lipid deposits per caudal vein segment. Mean ± SEM (12–21 animals in each group at each time point). *$P < 0.05$.

plement; therefore, the therapeutic effect of IK17-scFv would be limited to binding and blocking of MDA epitopes (as in Figure 5), resulting in inhibition of OxLDL binding and uptake by macrophages and reduced foam cell formation. The latter is believed to be a rate-limiting step in the development of atherosclerosis (3). Thus, because IK17 is able to reduce the accumulation of oxidation-specific epitopes in parallel with reduction of vascular lipid accumulation, and because probucol, a known antioxidant, also reduced oxidation-specific epitopes, these data strongly implicate lipoprotein oxidation as a quantitatively important event in the early vascular wall lipid accumulation that occurs in the HCD-fed zebrafish.

The majority of vascular lipid deposits and sites of IK17 binding in zebrafish larvae were located in the caudal vein (Figure 1B, Figure 3A, and Figure 4A; Supplemental Figures 1–3 and 9; and ref. 1). This is in contrast to the findings in adult zebrafish fed a HCD, in which vascular lesions occur only in the dorsal aorta and not in the caudal vein (1), as is found in mouse, rabbit, and human atherosclerotic lesions. There could be several reasons for the caudal vein localization of vascular lesions in zebrafish larvae 10 to 25 dpf. The dorsal aorta in zebrafish is a low-pressure artery, since the blood pumped by the heart is first directed to the gills' capillary network for oxygenation and only then collected into the dorsal aorta. Thus, in larvae, only a few lipid deposits are found in the dorsal aorta at sites of intersegmental artery bifurcation (1), in which turbulent flow is expected. Turbulent flow, an important factor in atherosclerotic lesion formation in mammalian arteries, is likely a major factor of lesion formation in the caudal vein of HCD-fed zebrafish at a larval stage. At this stage of development, the caudal vein has an irregular architecture, which likely includes sites of reduced shear stress and/or of turbulent flow (as shown in ref. 1 and Supplemental Figure 4). Even if the exact flow in the caudal vein is different from the flow patterns at bifurcations of major arteries in mammals, this apparently suffices, under conditions of hypercholesterolemia, to result in vascular lipid deposition.

The vein localization of lesions and other features of this new zebrafish model of vascular lipid accumulation and lipoprotein oxidation, as described in the current work and our other research papers (1, 2), underscore the importance of not over interpreting the results of zebrafish modeling studies. Each nonhuman model differs from the human experience. However, study of model systems allows us to uncover biological mechanisms underlying specific steps in the pathogenesis of human disease. The advent of genetic engineering pointed out that valuable lessons can be learned from mouse models of specific pathological processes of atherogenesis. In a similar manner, we suggest that this zebrafish model allows the study of specific and highly relevant pathological steps involved in early stages of development of lipoprotein oxidation and deposition in vascular beds. In the current manuscript, we studied vascular lipid deposition and accumulation of oxidation-specific epitopes in zebrafish — these are indeed relevant topics for development of human lesions, even if the eventual outcome of these lesions is different from that in humans.

Thus, in aggregate, the results of this study strongly support the use of the HCD-fed zebrafish in which controlled expression of oxidation-specific antibodies offers a specific and quantitative way to assess the extent of vascular accumulation of oxidation-specific epitopes. This useful model can allow the rapid initial screening of interventions that can inhibit LDL oxidation and/or uptake of OxLDL by macrophages. In addition, to the extent that oxidation of LDL is an important pathogenic event in humans (24), these studies suggest the possibility that oxidation-specific antibodies, such as the human IK17-scFv, can have an important role in a range of therapeutic applications in humans.

Methods

Zebrafish maintenance and feeding. Wild-type (AB) zebrafish embryos were obtained by in vitro fertilization, and natural spawning of adults was maintained at 28°C on a 14-hour-light/10-hour-dark cycle and staged as described previously (25). Zebrafish larvae were fed twice a day, starting at the fifth dpf, with either control diet (Golden Pearls, 100- to 200-μm size from Brine Shrimp Direct) or HCD (4% cholesterol added to Golden Pearls) for 5, 10, or 15 days, as described in our previous work (1). All animal studies were approved by the Animal Care and Use Committee of the UCSD.

Generation of IK17 and TT single-chain antibodies. The human Fab monoclonal antibody IK17 was cloned from a phage-display library, as previously described (7). The IK17 Fab was converted into a scFv fragment as described in ref. 13. In brief, VL and VH fragments were amplified using the following primers: forward 5′-GGGCCCAGGCGGCCGAGCTCGTGWTGACRCAGTCTCC and reverse 5′-GGAAGATCTAGAGGAACCACCTTTGATCTCCAGCTTGGTCCC for VL; and forward 5′-GGTGGTTCCTCTAGATCTTCCGAGGTGCAGCTGCTCGAGTCGGG and reverse 5′-CCTGGCCGGCCTGGCCACTAGTGACCGATGGGCCCTTGGTGGARGC for VH. The VL and VH products were then used to assemble the IK17-scFv with a VL-linker-VH structure. The coding region of IK17-scFv was amplified with primers (forward 5′-ACGAAGCTTGCTCGTGTTGACGCAGTCTCC and reverse 5′-CGAGCGGCCGCTGAGGAGACGGTGACCCGG) and subcloned into the eukaryotic expression vector pSecTag2A (Invitrogen), which provides a mouse kappa signal sequence for expression and secretion. The same strategy was used to engineer a TT-scFv, derived from a TT Fab, provided by Gregg Silverman (UCSD). The following primers were used: forward 5′-GGCCCAGGCGGCCGAGCTCACGCAGTCTCCAG and reverse 5′-GGAAGATCTAGAGGAACCACCTCGTTTGAGTTCCACCTTGG for VL; and forward 5′-GGTGGTTCCTCTAGATCTTCCGCCGAGGTGCAGCTGCTCGAGC and reverse 5′-CTGGCCGGCCTGGCCTGCGGAGACGGTGACCGTGGTCCC for VH. The TT-scFv was subcloned into the eukaryotic expression vector pSecTag2A using the following 2 primers: forward 5′-ACGAAGCTTGGCGGCCGAGCTCACGCAGTC and reverse 5′-CGAGCGGCCGCCTGGCCGGCCTGGCCTGCGGAG. The TT-scFv was amplified using the following 2 primers: forward 5′-GGGCTAGCCGCCACCATGGAGACAGAC (NheI) and reverse 5′-CCGGGATCCGCGTCGACGGCGCTATTCAG (BamHI) to provide restriction sites for subcloning into pEGFPN1.

Recombinant antibodies and zebrafish injections. Recombinant IK17-scFv and TT-scFv were grown in BL21 (DE3) *E. coli* cells (Invitrogen) and purified using an anti-HA affinity purification column (Sigma-Aldrich), followed by covalent labeling with Alexa Fluor 488 (Invitrogen) according to the manufacturer's protocol. As we found that endotoxin contamination dramatically increases vascular accumulation of injected antibodies, care was taken to remove endotoxin from the labeled antibody preparations using a Triton X114 extraction procedure (26). Two nl 10 ng/μl IK17-Alexa488 or TT-Alexa488 was injected intravenously into the posterior cardinal vein, as shown in Supplemental Figure 4. Twenty-four hours later, the zebrafish were imaged in the caudal vein area (Supplemental Figures 1 and 4), which was a different area from that of the site of injection.

Expression of IK17-EGFP and TT-EGFP in cell culture. IK17-scFv and TT-scFv with secretion signal were subcloned into pEGFP-N1 (Clontech) and transiently transfected into HEK293 cells with Lipofectamine 2000 (Invitrogen) according to the manufacturer's protocol. Ten hours after transfection, the transfection media were replaced with 1% FBS/DMEM, and the cell culture media were harvested 38 hours later and analyzed using microplate immunoassays.

Transgenic zebrafish. Vectors with the hsp70 promoter (15) were from David Traver (UCSD), and those for transposon-mediated zebrafish mutagenesis (mTol2) were from Koichi Kawakami (National Institute of Genetics, Mishima, Japan) (27). IK17-EGFP and TT-EGFP were excised from pEGFP-N1 using NheI and AflII, their overhangs were blunt ended using Klenow fragment and then ligated into mTol2-hsp70 (Figure 2B). Approximately 2 nl of a mix containing 50 ng/μl of the plasmid and 25 ng/μl of *transposase* mRNA (with 0.05% Phenol Red) was injected into 1-cell stage embryos to generate transgenic founders. Fish were maintained to adulthood and genotyped using IK17- or TT-specific primers to identify positive founders. F_1 and F_2 progeny were subjected to heat shock (1 hour at 37°C) to confirm EGFP expression. Embryos that were used for experiments were not subjected to heat shock until 48 hours before an imaging session.

In vivo confocal microscopy. Confocal microscopy of live anesthetized zebrafish larvae was performed as previously reported (1). Zebrafish were kept in a sealed, temperature-controlled chamber (20-20 Technology) in a small drop of 0.02% tricaine (Sigma-Aldrich) containing system water. A Nikon C1-si confocal microscope was used to detect fluorescence of Alexa Fluor 488 or EGFP (excitation 488 nm; green channel) and/or BODIPY 576/589 (excitation 561 nm; red channel). Z-stacks with a 1- to 3-μm step (512 × 512 focal planes, 40–100 μm in depth) were acquired over a 1- to 3-minute period using ×20 or ×63 objectives. Images were 3D rendered and analyzed using Imaris software (Bitplane).

Quantifying vascular lipid accumulation in larvae. Vascular lipid quantification was performed as detailed in our earlier work (1). Wild-type AB or transgenic *hsp70:IK17-GFP* or *hsp70:TT-GFP* larvae were fed a control diet or a 4% cholesterol HCD, starting on the fifth dpf. To visualize vascular lipid deposits, 2 days before an imaging session, both the control diet and the HCD were supplemented with 10 μg/g cholesteryl BODIPY 576/589 C11 (Invitrogen), a red fluorescent lipid marker. Images captured in the trunk/tail area (Supplemental Figures 1 and 4) and rendered using Imaris software were exported as TIFF files, and the area of a fluorescent signal was quantified using ImageJ software (http://rsbweb.nih.gov/ij/). Diffuse low-intensity fluorescence of BODIPY 576/589 (likely carried by plasma lipoproteins) marked the lumen of a blood vessel. The area of a blood vessel segment was measured to serve as a denominator for normalization. The intensity in the lumen was set as a threshold value for quantifying vascular lipid accumulation — all focal sites with intensity above the threshold were counted as vascular wall lipid deposits as described previously (1). The area of lipid deposits was normalized by the area of a vascular segment.

Quantifying vascular binding of IK17-EGFP and TT-EGFP in larvae. After capturing EGFP fluorescence and image rendering, the area of EGFP signals in the caudal vein that colocalized with red lipid deposits was quantified using ImageJ (http://rsbweb.nih.gov/ij/) and normalized to the area of a blood vessel segment as described above. The absolute numbers for lipid deposit area were in the range of 384–1536 μm^2 per caudal vein, and those for IK17-EGFP binding were in the range of 38–576 μm^2. These measurements are feasible with a ×20 objective of the confocal microscope (note scale bars in images). We observed up to 10-fold differences in IK17 binding between different zebrafish and quantified 11–34 animals for each data point. The percentages of zebrafish vascular lesions per total caudal vein area (2%–8% for lipid deposits and 0.2%–3.0% for IK17 binding) are consistent with the size of atherosclerotic lesions in the whole aorta of *Ldlr*$^{-/-}$ mice receiving a HCD. Note that in some larvae, at 10 to 15 dpf, pigmented cells in the skin, which display wide-spectrum fluorescence, locate too close to the vasculature and interfere with accurate confocal imaging. These zebrafish were excluded from the analysis.

Modification of LDL. LDL (density = 1.019–1.063 g/ml) was isolated from pooled plasma of healthy donors by sequential ultracentrifugation (28). To produce OxLDL, LDL (0.1 mg/ml) was incubated with 10 μM $CuSO_4$ for 18 hours at 37°C. The extent of LDL oxidation was assessed by measuring thiobarbituric acid–reactive substances (typically, more than 30 nmol/mg protein in OxLDL) (29). MDA-LDL was prepared by incubating LDL with freshly made 0.5 M MDA, generated from malonaldehyde bis(dimethylacetyl) (Sigma-Aldrich) by acid hydrolysis (30). The degree of MDA modification determined by the picrylsulfonic acid method (TNBS) averaged 77% lysine residues.

Zebrafish homogenates for immunoassays. At the end of the feeding period, 20–50 zebrafish larvae in each experimental group were euthanized by prolonged exposure to tricaine. Abdomens containing undigested food were removed, and the remaining bodies were pooled and homogenized in 200 μl ice-cold PBS containing 10 μM butylated hydroxytoluene (an antioxidant added to prevent ex vivo oxidation) in an eppendorf tube using a plastic pestle. The resultant homogenates were filtered through a sterile 0.45-μm Millex-HV membrane filter (Millipore). Protein content in the homogenates was determined using the Bradford assay with the BCA Protein Assay (Pierce).

Microplate immunoassays. Binding of IK17-EGFP and of IK17-Alexa488 (and corresponding TT controls) to MDA-LDL and Cu-OxLDL was determined using microplate immunoassays with chemiluminescence detection, as described previously (12). Plates were coated with native LDL, MDA-LDL, or Cu-OxLDL, and supernatants of HEK293 cells (transfected with IK17-EGFP or TT-EGFP) or fish homogenates (from *hsp70:IK17-EGFP* or *hsp70:TT-EGFP* larvae subjected to heat shock) were added. Binding was detected with antibodies to GFP (Novus Biologicals) or to HA (Sigma-Aldrich) labeled with alkaline phosphatase (AP), followed by addition of the AP substrate LumiPhos 530 (Lumigen). The resulting light emission was measured as RLUs over 100 ms using a Dynex Luminometer (Dynex Technologies).

Antibody K_d measurements. The apparent affinities of IK17 Fab and of IK17-EGFP expressed in zebrafish homogenates binding to MDA-LDL were determined by a competitive inhibition assay, as described previously (7, 31). Purified IK17 Fab (2.5 μg/ml) or homogenates of *hsp70:IK17-EGFP* zebrafish (subjected to heat shock on the second and then fourth dpf and harvested on the fifth dpf; 0.6 mg/ml) were preincubated in the absence or presence of 6 to 200 μg/ml MDA-LDL and then added to microtiter plates coated with 5 μg/ml MDA-LDL. Recombinant EGFP was used as a negative control for IK17-EGFP binding to MDA-LDL. A chemiluminescent immunoassay was performed as above, with AP-labeled anti-human IgG (Fab specific) or anti-GFP antibodies to detect IK17 Fab or IK17-EGFP binding, respectively. This assay allows measurement of apparent antibody dissociation constants in impure preparations (31), such as a zebrafish larvae homogenate. A molecular weight of 500,000 Da (apoB-100) was used for calculating the molar concentration of MDA-LDL.

Macrophage binding and competition assays. A 96-well microplate chemiluminescent assay to characterize binding of biotinylated MDA-LDL to J774 murine macrophages has been previously described by our group (6). Here, we used this assay to demonstrate that IK17 and homogenates of HCD-fed zebrafish larvae harboring the IK17 transgene compete with MDA-LDL for macrophage binding. In brief, J774 macrophages were plated in microtiter plates and subsequently incubated overnight at 4°C with 0.15 μg/ml biotinylated MDA-LDL in the absence or presence of competitors, including IK17-scFV or TT-scFv, or homogenates of transgenic zebrafish subjected or not subjected to heat shock. The extent of MDA-LDL binding was then detected with NeutrAvidin-conjugated AP (Pierce), LumiPhos 530, and a Dynex Luminometer. Data were expressed as a ratio of binding in the presence of competitor (B) divided by binding in the absence of competitor (B_0).

Immunohistochemistry. A protocol for preparation of frozen sections of trunk/tail segments of adult zebrafish has been described in our previous work (1). EDTA and BHT were added to prevent ex vivo oxidation. To stain oxidation-specific epitopes, the tissue sections were thawed and washed

3 times with PBS to remove OCT. After blocking with 1% BSA in TBS, the sections were incubated with 1 μg/ml IK17-Alexa488 in 1% BSA/TBS. The slides were mounted with Prolong Gold mounting media containing DAPI for nuclear staining (Invitrogen). Images were captured with a Leica CTR5000 fluorescent microscope, equipped with a Leica DC500 camera.

Statistics. Two-way ANOVA with Bonferroni post-hoc test was used to analyze time course/treatment experiments (Figure 3, B and C; Figure 4, B and C; and Figure 6B). Student's *t* test (2 tailed) was used to analyze differences between means of 2 groups (Figure 6A). $P < 0.05$ was used as the significance threshold.

Study approval. Animal studies were approved by the Institutional Animal Care and Use Committees at UCSD.

Acknowledgments

We thank David Traver, Richard Klemke, and Konstantin Stoletov (UCSD) and Koichi Kawakami (National Institute of Genetics, Japan) for many helpful discussions and/or for providing reagents and access to equipment for this study as well as Felicidad Almazan, Jennifer Pattison, and Tiffany Sayaphupha for excellent technical assistance. This study was supported by NIH grants HL093767 (to Y.I. Miller and L. Fang), HL086559 (to J.L. Witztum), and HL0888093 (to Y.I. Miller, S. Tsimikas, and J.L. Witztum); fellowship 18FT-0137 from the UC Tobacco-Related Disease Program (to L. Fang); Pilot Innovative Technology grant from UCSD Clinical and Translational Research Institute (to Y.I. Miller); and a grant from the Leducq Fondation (to J.L. Witztum, S. Tsimikas, and Y.I. Miller). Walter and Eliza Hall Institute of Medical Research receives infrastructure support from the Commonwealth NHMRC Independent Research Institutes Infrastructure Support Scheme (361646) and a Victorian State Government Operational Infrastructure Support Scheme grant (to F. Ellett and G.J. Lieschke). The Australian Regenerative Medicine Institute is supported by grants from the State Government of Victoria and the Australian Government (to F. Ellett and G.J. Lieschke).

Received for publication June 7, 2011, and accepted in revised form October 12, 2011.

Address correspondence to: Yury I. Miller, Department of Medicine, University of California, San Diego, 9500 Gilman Drive, La Jolla, California 92093, USA. Phone: 858.822.5771; Fax: 858.534.2005; E-mail: yumiller@ucsd.edu.

1. Stoletov K, et al. Vascular lipid accumulation, lipoprotein oxidation, and macrophage lipid uptake in hypercholesterolemic zebrafish. *Circ Res*. 2009;104(8):952–960.
2. Fang L, et al. Oxidized cholesteryl esters and phospholipids in zebrafish larvae fed a high–cholesterol diet: macrophage binding and activation. *J Biol Chem*. 2010;285(42):32343–32351.
3. Glass CK, Witztum JL. Atherosclerosis. The road ahead. *Cell*. 2001;104(4):503–516.
4. Nishi K, et al. Oxidized LDL in carotid plaques and plasma associates with plaque instability. *Arterioscler Thromb Vasc Biol*. 2002;22(10):1649–1654.
5. Miller YI, et al. Oxidation–specific epitopes are danger associated molecular patterns recognized by pattern recognition receptors of innate immunity. *Circ Res*. 2011;108(2):235–248.
6. Chou MY, et al. Oxidation-specific epitopes are dominant targets of innate natural antibodies in mice and humans. *J Clin Invest*. 2009;119(5):1335–1349.
7. Shaw PX, et al. Human-derived anti-oxidized LDL autoantibody blocks uptake of oxidized LDL by macrophages and localizes to atherosclerotic lesions in vivo. *Arterioscler Thromb Vasc Biol*. 2001; 21(8):1333–1339.
8. Briley-Saebo KC, et al. Targeted molecular probes for imaging atherosclerotic lesions with magnetic resonance using antibodies that recognize oxidation-specific epitopes. *Circulation*. 2008;117(25):3206–3215.
9. Briley-Saebo KC, et al. Targeted iron oxide particles for in vivo magnetic resonance detection of atherosclerotic lesions with antibodies directed to oxidation-specific epitopes. *J Am Coll Cardiol*. 2011; 57(3):337–347.
10. Palinski W, Miller E, Witztum JL. Immunization of low density lipoprotein (LDL) receptor-deficient rabbits with homologous malondialdehyde-modified LDL reduces atherogenesis. *Proc Natl Acad Sci U S A*. 1995;92(3):821–825.
11. Freigang S, Horkko S, Miller E, Witztum JL, Palinski W. Immunization of LDL receptor deficient mice with homologous malondialdehyde-modified and native ldl reduces progression of atherosclerosis by mechanisms other than induction of high titers of antibodies to oxidative neoepitopes. *Arterioscler Thromb Vasc Biol*. 1998;18(12):1972–1982.
12. Binder CJ, et al. Pneumococcal vaccination decreases atherosclerotic lesion formation: molecular mimicry between Streptococcus pneumoniae and oxidized LDL. *Nat Med*. 2003;9(6):736–743.
13. Tsimikas S, et al. Human oxidation-specific antibodies reduce foam cell formation and atherosclerosis progression. *J Am Coll Cardiol*. 2011; 58(16):1715–1727.
14. Ellett F, Pase L, Hayman JW, Andrianopoulos A, Lieschke GJ. mpeg1 promoter transgenes direct macrophage-lineage expression in zebrafish. *Blood*. 2011; 117(4):e49–e56.
15. Halloran MC, et al. Laser-induced gene expression in specific cells of transgenic zebrafish. *Development*. 2000;127(9):1953–1960.
16. Parthasarathy S, Young SG, Witztum JL, Pittman RC, Steinberg D. Probucol inhibits oxidative modification of low density lipoprotein. *J Clin Invest*. 1986;77(2):641–644.
17. Carew TE, Schwenke DC, Steinberg D. Antiatherogenic effect of probucol unrelated to its hypocholesterolemic effect: evidence that antioxidants in vivo can selectively inhibit low density lipoprotein degradation in macrophage-rich fatty streaks and slow the progression of atherosclerosis in the Watanabe heritable hyperlipidemic rabbit. *Proc Natl Acad Sci U S A*. 1987;84(21):7725–7729.
18. Binder CJ, et al. IL-5 links adaptive and natural immunity specific for epitopes of oxidized LDL and protects from atherosclerosis. *J Clin Invest*. 2004; 114(3):427–437.
19. Babin PJ, Vernier JM. Plasma lipoproteins in fish. *J Lipid Res*. 1989;30(4):467–489.
20. Schlegel A, Stainier DYR. Microsomal triglyceride transfer protein is required for yolk lipid utilization and absorption of dietary lipids in zebrafish larvae. *Biochemistry*. 2006;45(51):15179–15187.
21. Jin S, Cho KH. Water extracts of cinnamon and clove exhibits potent inhibition of protein glycation and anti–atherosclerotic activity in vitro and in vivo hypolipidemic activity in zebrafish. *Food Chem Toxicol*. 2011;49(7):1521–1529.
22. Tsimikas S, Shortal BP, Witztum JL, Palinski W. In vivo uptake of radiolabeled MDA2, an oxidation-specific monoclonal antibody, provides an accurate measure of atherosclerotic lesions rich in oxidized LDL and is highly sensitive to their regression. *Arterioscler Thromb Vasc Biol*. 2000;20(3):689–697.
23. Steinberg D. The LDL modification hypothesis of atherogenesis: an update. *J Lipid Res*. 2009; 50(suppl):S376–S381.
24. Tsimikas S, Miller YI. Oxidative modification of lipoproteins: mechanisms, role in inflammation and potential clinical applications in cardiovascular disease. *Curr Pharm Des*. 2011;17(1):27–37.
25. Kimmel CB, Ballard WW, Kimmel SR, Ullmann B, Schilling TF. Stages of embryonic development of the zebrafish. *Dev Dyn*. 1995;203(3):253–310.
26. Liu S, Tobias R, McClure S, Styba G, Shi Q, Jackowski G. Removal of endotoxin from recombinant protein preparations. *Clin Biochem*. 1997;30(6):455–463.
27. Nagayoshi S, et al. Insertional mutagenesis by the Tol2 transposon-mediated enhancer trap approach generated mutations in two developmental genes: tcf7 and synembryn-like. *Development*. 2008; 135(1):159–169.
28. Havel RJ, Bragdon JH, Eder HA. The distribution and chemical composition of ultracentrifugally separated lipoproteins in human serum. *J Clin Invest*. 1955;34(9):1345–1353.
29. Boullier A, et al. Minimally oxidized LDL offsets the apoptotic effects of extensively oxidized LDL and free cholesterol in macrophages. *Arterioscler Thromb Vasc Biol*. 2006;26(5):1169–1176.
30. Ylä-Herttuala S, et al. Evidence for the presence of oxidatively modified low density lipoprotein in atherosclerotic lesions of rabbit and man. *J Clin Invest*. 1989;84(4):1086–1095.
31. Friguet B, Chaffotte AF, Djavadi-Ohaniance L, Goldberg ME. Measurements of the true affinity constant in solution of antigen-antibody complexes by enzyme-linked immunosorbent assay. *J Immunol Methods*. 1985;77(2):305–319.